Available online at www.sciencedirect.com
SCIENCE DIRECT®
Journal of Power Sources 146 (2005) 275–280
JOURNAL OF POWER SOURCES
www.elsevier.com/locate/jpowsour

Overcharging manganese oxides: Extracting lithium beyond Mn^{4+}

A.R. Armstrong *, A.D. Robertson, P.G. Bruce

School of Chemistry, University of St. Andrews, St. Andrews, Fife KY16 9 ST, UK

Available online 13 June 2005

Abstract

It has been demonstrated previously that Li may be removed electrochemically from Mn containing oxides beyond the maximum oxidation state of 4+ for Mn in an octahedral oxygen environment. Here we present a comparison of such overcharge behavior in a series of different layered lithium manganese oxides including Li_2MnO_3, $Li_x[Mn_{1-y}Li_y]O_2$, ($y \leq 0.2$), and $Li[Ni_xLi_{1/3-2x/3}Mn_{2/3-x/3}]O_2$ ($0 \leq x \leq 0.5$). We show that there are two competing mechanisms by which electrochemical extraction of lithium can occur in Mn (4+) systems. In the first Li removal is accompanied by O^{2-} loss (effective removal of Li_2O) whilst the second involves oxidation of the non-aqueous electrolyte thus generating H^+ ions which exchange for Li^+. At 30 °C the first mechanism is dominant in all examples studied, whilst at 55 °C the proton exchange mechanism becomes more important. At 30 °C H^+ exchange is more prevalent in Li_2MnO_3 than in the other two cases. The preference for O loss in the Mn/Ni system may be understood in terms of the ease with which MnO_2 will lose oxygen.

Keywords: Lithium manganese oxide; Octahedral; Proton exchange mechanism

1. Introduction

The inability to oxidise Mn beyond Mn^{4+} in an octahedral oxygen environment was thought to limit the quantity of Li that may be removed and led to the widespread belief that oxides containing Mn^{4+} were electrochemically inactive [1,2]. As a result, Mn^{4+} compounds such as Li_2MnO_3 (which adopts a layered structure $Li[Li_{1/3}Mn_{2/3}]O_2$), despite being rich in mobile Li^+ ions, were considered electrochemically inert. Recently, however, electrochemical removal of Li beyond the Mn^{4+} limit has been discussed. Charge compensation by oxidation of Mn^{4+} to Mn^{5+} has been proposed [3]. However, a more likely explanation has been advanced by Dahn et al. based on oxygen loss [4,5]. Such additional capacity to deliver Li could have important repercussions for use of lithium manganese oxides in rechargeable lithium batteries.

In order to investigate this phenomenon further we have studied the electrochemical behavior of the layered compounds Li_2MnO_3, $Li_x[Mn_{1-y}Li_y]O_2$, ($y \leq 0.2$), and $Li[Ni_xLi_{1/3-2x/3}Mn_{2/3-x/3}]O_2$ ($0 \leq x \leq 0.5$) all having the O3 structure (ABC oxygen stacking). As they adopt a layered structure, the Li^+ ions are expected to be mobile and hence any limit on the ability to extract lithium must be due to other factors.

By using a range of techniques including chemical analysis, combined thermogravimetric analysis and mass spectroscopy (TG–MS, in which the gases evolved during heating are analysed using a mass spectrometer) and XPS, we have been able to identify the processes involved in the overcapacity (Li removal beyond Mn^{4+}) of each of these systems, both at 30 and 55 °C. In addition, powder neutron diffraction studies on $Li_x[Mn_{1-y}Li_y]O_2$ at various states of charge have enabled the identification of the various phases and provided confirmation of the proposed mechanisms of lithium extraction.

In each of these systems two mechanisms of electrochemical Li removal are found to operate beyond the Mn^{4+} limit. These are the loss of oxygen (effective removal of Li_2O) as proposed by Dahn [5–7], and proton exchange for Li^+, in which the protons are generated by the oxidation of the non-aqueous electrolyte [8,9]. The interplay between these mechanisms is subtly dependent on the conditions. Presenting the

* Corresponding author.
E-mail address: ara@st-andrews.ac.uk (A.R. Armstrong).

0378-7753/$ – see front matter © 2005 Elsevier B.V. All rights reserved.
doi:10.1016/j.jpowsour.2005.03.104

results for these three systems in one paper facilitates comparison between them. The three systems vary in their complexity. In the case of Li_2MnO_3 the ratio of Li:Mn on the transition metal sites is fixed at 1:2 whereas in $Li_xMn_{1-y}Li_yO_2$ it varies with y and in the case of $Li[Ni_xLi_{1/3-2x/3}Mn_{2/3-x/3}]O_2$ a second transition metal is introduced. These variations have a profound effect on the balance between H^+ exchange and O loss with consequent differences in the capacity and reversibility of Li intercalation.

The phenomenon of overcapacity is an important one. Although the mechanism by which extra lithium ions are removed from such materials may be irreversible (H^+ exchange or O loss), the capacity of the materials to reversibly reinsert lithium increases by their removal (if the mechanism is predominantly O loss). In other words, on charging these materials although some of the lithium is initially removed by an irreversible mechanism, this quantity of lithium may subsequently be reinserted by a reversible mechanism (involving reduction of Mn^{4+} to Mn^{3+}). Therefore, the capacity of the material reversibly to store lithium is increased.

2. Experimental

The synthesis of Li_2MnO_3, $Li_xMn_{1-y}Li_yO_2$ ($y \leq 0.2$) and $Li[Ni_xLi_{1/3-2x/3}Mn_{2/3-x/3}]O_2$ ($x = 0.15$) have been described previously and will only be summarised here [5–11]. Li_2MnO_3 was prepared by solid state reaction between Li_2CO_3 and $MnCO_3$ at 500 °C for 40 h, with an intermediate grinding. The $Li[Ni_xLi_{1/3-2x/3}Mn_{2/3-x/3}]O_2$ ($x = 0.15$) composition was prepared by the "mixed hydroxide" method described by Lu et al. [5–7]. $Li_xMn_{1-y}Li_yO_2$ ($y \leq 0.2$) materials were prepared by ion exchange from the corresponding sodium phase by refluxing in ethanol at 80 °C with a 7–8-fold molar excess of LiBr for up to 8 h. The products were then filtered, washed and dried.

Chemical analyses for sodium and lithium were carried out by flame emission and for manganese using atomic absorption spectroscopy. The average transition metal oxidation state was determined by redox titration using ferrous ammonium sulfate/$KMnO_4$. Further information on the manganese oxidation state was obtained from XPS measurements on as-prepared and charged composite electrodes. Binding energies were charge corrected using the C_{1s} peak (284.4 eV).

Powder X-ray diffraction data were collected on a Stoe STADI/P diffractometer operating in transmission mode with Fe $K\alpha_1$ radiation ($\lambda = 1.936$ Å) to eliminate manganese fluorescence. Powder neutron diffraction experiments were carried out on charged samples on the GEM diffractometer at ISIS, Rutherford Appleton Laboratory. The samples were contained in 2 mm quartz capillaries. The structures were refined by the Rietveld method using the program Prodd based on the Cambridge Crystallographic Subroutine Library (CCSL) [12,13]. Scattering lengths of -0.19×10^{-12}, -0.373×10^{-12}, and 0.5803×10^{-12} cm were assigned to Li, Mn, and O, respectively [14].

Electrochemical measurements were made using two-electrode coin cells comprising a lithium manganese oxide working electrode and Li metal counter electrode. The electrolyte was either a 1 molal solution of $LiPF_6$ in EC:DMC (1:1) (Merck) or 1 molal $LiPF_6$ (Hashimoto) in ethylene carbonate/diethyl carbonate 1:2 (V/V (Merck)). Li_2MnO_3 electrodes were fabricated either as composite electrodes for extended galvanostatic cycling experiments or as pressed pellets. The composite electrodes were formed by casting a mixture of the active material, Super S carbon and Kynar Flex 2801 binder in the weight ratios 75:17:8, onto Al foil. In the case of $Li[Ni_xLi_{1/3-2x/3}Mn_{2/3-x/3}]O_2$ and $Li_xMn_{1-y}Li_yO_2$ electrodes this ratio was 85:10:5. After the solvent had evaporated the foils were pressed and 1.3 cm discs were cut. The pressed pellets were prepared by mixing active material with graphite in the weight ratios 80:20 then cold pressing. Electrochemical measurements were carried out at 30 and 55 °C using a Biologic Macpile II. Charge–discharge curves of cells containing composite electrodes and pressed pellets were compared to ensure reproducibility. After cycling, cells were transferred to an argon-filled glove box and the active material removed. The electrodes were then rinsed with a small amount of dry solvent to remove residual electrolyte and dried under dynamic vacuum overnight.

TG–MS measurements were performed using a Netzsch STA449 Jupiter instrument coupled with a Pfeiffer Vacuum Thermostar GSD300T. The TGA heating rate was 5 °C min^{-1} up to 400 °C under an argon atmosphere.

3. Results and discussion

3.1. Li_2MnO_3

The variation of voltage with capacity for the first cycle in Li_2MnO_3 is shown in Fig. 1. Significant charge may be removed at both 30 and 55 °C and this process is also partially reversible. The amount of lithium removed and reinserted was

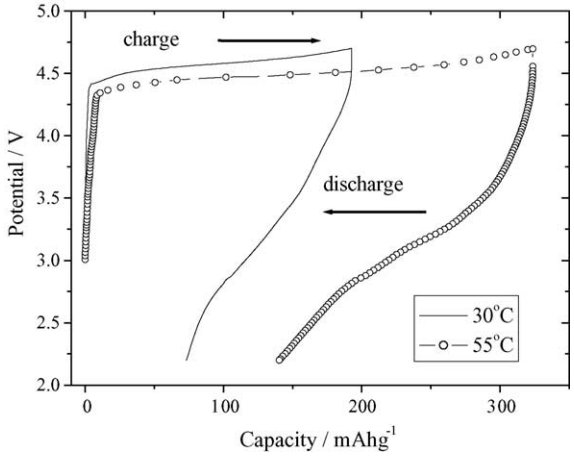

Fig. 1. First charge–discharge curves for Li_2MnO_3 vs. Li^+(1 M)/Li. Rate = 10 mA g^{-1}.

Table 1
Analysis of electrochemically delithiated-relithiated Li_2MnO_3 (FE, AAS, XPS, TGA–MS)

Preparative conditions	Observed composition Li:Mn ratio (FE/AAS)	Theoretical Li:Mn ratio based on quantity of charge passed	Av. Mn valence (XPS)	H content (TGA–MS)	Proposed bulk composition
OCV 55 °C, 48 h	$Li_{1.89}Mn_{1.00}$	$Li_{2.00}Mn_{1.00}$	4+	$H_{0.20}$	$Li_{1.89}H_{0.20}MnO_{3.04}$
1st Charge, 55 °C, −309 mA h g^{-1}	$Li_{0.62}Mn_{1.00}$	$Li_{0.65}Mn_{1.00}$	4+	$H_{1.29}$	$Li_{0.62}H_{1.29}MnO_{2.95}$
1st Charge, 55 °C, −199 mA h g^{-1}	$Li_{1.07}Mn_{1.00}$	$Li_{1.13}Mn_{1.00}$	4+	$H_{0.86}$	$Li_{1.07}H_{0.86}MnO_{2.97}$
1st Charge, 30 °C, −235 mA h g^{-1}	$Li_{0.87}Mn_{1.00}$	$Li_{0.97}Mn_{1.00}$	4+	$H_{0.64}$	$Li_{0.87}H_{0.64}MnO_{2.76}$
1st Charge, 30 °C, −199 mA h g^{-1}	$Li_{1.04}Mn_{1.00}$	$Li_{1.13}Mn_{1.00}$	4+	$H_{0.41}$	$Li_{1.04}H_{0.41}MnO_{2.73}$
1st Charge, 30 °C, −92 mA h g^{-1}	$Li_{1.63}Mn_{1.00}$	$Li_{1.60}Mn_{1.00}$	4+	$H_{0.14}$	$Li_{1.63}H_{0.14}MnO_{2.89}$
1st discharge, 55 °C, −309 mA h g^{-1} then +125 mA h g^{-1}	$Li_{1.28}Mn_{1.00}$	$Li_{1.20}Mn_{1.00}$	4+	$H_{0.66}$	$Li_{1.28}H_{0.66}MnO_{2.97}$

commensurate with the charge passed. At 55 °C thermogravimetric analysis, in which the evolved gases were analysed by mass spectrometry, indicated a substantial proton content after charging, and this was in excellent agreement with both the charge passed and lithium extracted (Table 1). X-ray powder diffraction at the end of charge revealed both the O3 structure of Li_2MnO_3 as well as a P3 structure, Fig. 2. The former corresponds to ABC stacking of O^{2-} layers whereas the latter corresponds to AABBCC stacking (CrOOH structure type). The driving force for adoption of the P3 structure is hydrogen bonding between adjacent oxide ion layers. The most likely explanation for electrochemical activity of Li_2MnO_3 at 55 °C is electrogeneration of H^+ followed by exchange with Li^+ in the electrode. It has been shown previously that PF_6^- based electrolytes contain H^+ due to the formation of HF. Furthermore at a voltage of 4.5 V versus Li^+ (1 M)/Li more H^+ may be electrochemically generated adding further weight to this interpretation [15].

At 30 °C, as at 55 °C, the amount of Li removal on charge is in agreement with the charge passed. TG–MS results indicate the presence of H^+ in the material but unlike the behavior at 55 °C not all the Li^+ lost is replaced by H^+. As seen in Table 1

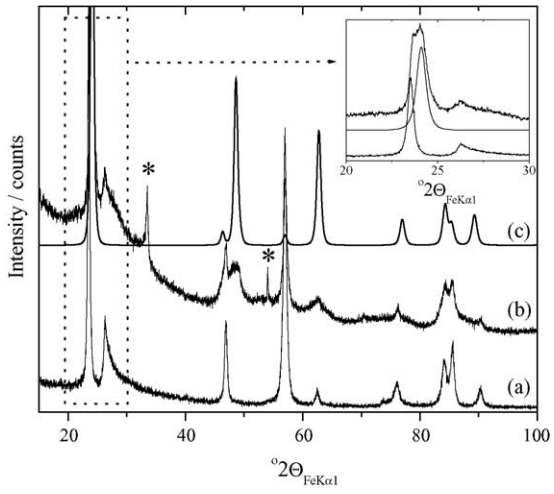

Fig. 2. Powder X-ray diffraction data for (a) as-synthesised Li_2MnO_3; (b) Li_2MnO_3-based electrode after electrochemical extraction of 1.35 Li and (c) simulated P_3 pattern for a delithiated sample, space group R3m, a = 2.885Å, c = 13.91 Å. Note* = graphite in (b).

there is evidence of some oxygen deficiency. Approximately 60% of the Li removed is replaced by H^+, the rest being charge compensated by O^{2-} loss. On extracting less charge (199 mA h g^{-1}) at 30 °C, it is evident from Table 1 that again two mechanisms, H^+ exchange and O^{2-} removal, operate. Despite removing less charge (199 instead of 235 mA h g^{-1}) the amount of oxygen lost is very similar. As a result, the proportion of Li removed that is balanced by H^+ exchange has dropped to around 45%. If only a small amount of charge is extracted (92 mA h g^{-1}) the proportion of H^+ to O loss is somewhat lower at 38%. It appears that on initial extraction of Li during charging at 30 °C, O^{2-} is removed, however, as more Li is removed this mechanism of charge compensation gives way to H^+ exchange. We may conclude that both mechanisms operate at 30 °C but H^+ exchange still dominates at high levels of Li extraction. The difference that raising the temperature has on the behavior is especially evident when comparing the two electrodes from which the same quantity of charge (199 mA h g^{-1}) was removed but at 30 and 55 °C, respectively, Table 1. At the lower temperature oxygen loss and H^+ exchange occurs whereas at 55 °C only H^+ exchange occurs. Thackeray et al. have studied Li_2MnO_3 oxidation in aqueous acid and observe H^+ exchange and O loss depending on the conditions used [16].

3.2. $Li(Ni_xLi_{1/3-2x/3}Mn_{2/3-x/3})O_2$ $[0 \le x \le 0.5]$

In layered Li-Ni-Mn-O, the oxidation states of Ni and Mn are respectively, 2+ and 4+. The materials may most usefully be described based on Li_2MnO_3, $Li[Li_{1/3}Mn_{2/3}]O_2$, in which $1Mn^{4+}$ and $2Li^+$ ions are replaced by $3Ni^{2+}$ ions thus generating the solid solution $Li[Ni_xLi_{1/3-2x/3}Mn_{2/3-x/3}]O_2$, $0 \le x \le 0.5$ [6]. An alternative description has been proposed by Thackeray et al. i.e. xLi_2MnO_3:$yLiNiO_2$ [17]. XANES measurements have shown that lithium may be extracted from such materials accompanied by oxidation of Ni^{2+} to Ni^{4+} [18]. The ability of these materials to demonstrate "overcharge" beyond Mn^{4+} involving the removal of lithium has been reported previously [5]. We have applied the TG–MS technique to $Li[Li_{0.23}Ni_{0.15}Mn_{0.62}]O_2$ (x = 0.15). As observed for Li_2MnO_3, it is evident from Table 2 that the charged $Li_y[Ni_xLi_{1/3-2x/3}Mn_{2/3-x/3}]O_2$ materials do contain some protons. Therefore, some Li removed from these

Table 2
$Li(Ni_x\ Li_{1/3-2x/3}\ Mn_{2/3-2x/3})O_2$ ($x = 0.15$) delithiation-relithiation chemical analysis results (FE, AAS, TGA–MS, redox titration)

Sample	Observed Li:Ni:Mn ratio (FE/AAS)	Theoretical Li:Ni:Mn ratio based on quantity of charge passed	Av. TM valence (redox tit.)	H content (TGA–MS)	Proposed bulk composition	Ratio of Li lost by O removal: Li lost by H exchange
As-prepared	$Li_{1.22}Ni_{0.14}Mn_{0.62}$	$Li_{1.23}Ni_{0.15}Mn_{0.62}$	3.66+		$Li_{1.22}Ni_{0.14}Mn_{0.62}O_2$	–
OCV 30 °C, 72 h	$Li_{1.22}Ni_{0.15}Mn_{0.62}$	$Li_{1.23}Ni_{0.15}Mn_{0.62}$	–	$H_{0.08}$	$Li_{1.22}Ni_{0.15}Mn_{0.62}O_2$; $0.04H_2O$	–
1st Charge, 30 °C, −299 mA h g^{-1}	$Li_{0.37}Ni_{0.15}Mn_{0.62}$	$Li_{0.30}Ni_{0.15}Mn_{0.62}$	–	$H_{0.10}$	$Li_{0.37}H_{0.10}$; $Ni_{0.15}Mn_{0.62}O_{1.78}$*	4.40:1
1st Charge, 55 °C, −187 mA h g^{-1}	$Li_{0.69}Ni_{0.15}Mn_{0.62}$	$Li_{0.65}Ni_{0.15}Mn_{0.62}$	–	$H_{0.068}$	$Li_{0.69}H_{0.068}$; $Ni_{0.15}Mn_{0.62}O_{1.92}$*	2.35:1
1st Charge, 55 °C, −331 mA h g^{-1}	$Li_{0.23}Ni_{0.15}Mn_{0.62}$	$Li_{0.20}Ni_{0.15}Mn_{0.62}$	–	$H_{0.17}$	$Li_{0.23}H_{0.17}$; $Ni_{0.15}Mn_{0.62}O_{1.74}$*	3.06:1

Note: *For delithiated materials, the quantity of protons in the proposed stoichiometries have been corrected to take into account the number of protons in the OCV sample.

electrodes have been replaced by H^+ from the electrolyte. An electrode maintained at OCV for an equivalent period showed only a small amount of H_2O and this was evolved at a lower temperature than the charged materials – we associate this with a small amount of surface adsorbed moisture. The quantity of H in this material was used to correct the H content of the delithiated samples. At 30 °C the dominant mechanism compensating for loss of lithium is simultaneous oxygen removal (Table 2). The ratio of lithium removed via oxygen loss to that of H^+ exchange is 4.40:1. Removing a similar quantity of charge at 55 °C results in greater H^+ exchange, with this ratio dropping to 3.06:1. There is no evidence of a P3 phase with $Li[Ni_xLi_{1/3-2x/3}Mn_{2/3-x/3}]O_2$ comensurate with the dominance of O loss over H^+ exchange.

3.3. $Li_x(Mn_{1-y}Li_y)O_2$ $[0 \le y \le 0.2]$

Li_2MnO_3 ($Li[Li_{1/3}Mn_{2/3}]O_2$) is the end member of a solid solution beginning with layered $LiMnO_2$ and involving replacement of Mn in the transition metal layers by Li. We might therefore expect similar electrochemical behavior for $Li_xMn_{1-y}Li_yO_2$ to Li_2MnO_3 once the lithium has been extracted by conventional oxidation of manganese up to 4+. Fig. 3 presents the variation of voltage with state of charge on the first cycle. In each case the charging curves are characterised by two distinct regions; an increasing potential on initial lithium extraction and then a plateau at approximately 4.5 V. With increasing Li doping the capacity associated with the rising potential decreases at the expense of an increasing capacity associated with the plateau. The first stage of electrochemical reaction involves a conventional Li^+ deintercalation with oxidation of Mn^{3+} to Mn^{4+}, as confirmed by chemical analysis and amount of charge passed.

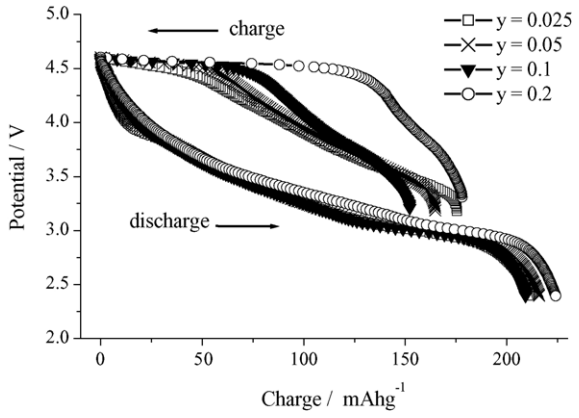

Fig. 3. Variation of potential (vs. Li^+[1 M]/Li) on charging then discharging the $Li_x[Mn_{1-y}Li_y]O2$ electrodes at 25 mA g^{-1} (C/8) and 30 °C.

In order to investigate how the charge associated with the 4.5 V plateau is removed we analysed electrodes at the end of charge for the 10 and 20% Li doped materials, Table 3. Again XPS measurements indicate that Mn remains 4+, with no evidence that O^{2-} has been oxidised. Based on the amount of Li removed at 4.5 V theoretical capacities were calculated and are in good agreement with the capacities observed to be associated with the 4.5 V plateau, Fig. 2, confirming that the charge extracted at 4.5 V has resulted in a corresponding amount of Li being removed from the electrode.

TG–MS results for the 10 and 20% doped materials indicate that protons do exchange for Li^+, as observed for Li_2MnO_3, however the amount of Li removed exceeds the amount of H^+ present in the electrodes. The difference is accounted for by oxygen loss (effective removal of Li_2O). In both cases Li removal via O loss is greater than by H exchange, indicating that the former mechanism dominates. Electrodes removed from cells before the onset of the 4.5 V plateau showed no evidence of H^+ exchange, nor did samples left at open circuit for several days.

The charging curve for the $y = 0.2$ material at 55 °C taken to a cut-off voltage of 4.8 V, is shown in Fig. 4. Chemical, oxidation state and TG/MS analysis of the electrode material at the end of charge yielded a composition $Li_{0.17}H_{0.19}Mn_{0.82}O_{1.82}$. The amount of Li removed corresponds to 220 mA h g^{-1}, in good agreement with the charge extracted (214 mA h g^{-1}). Comparing this composition with that for the same material charged at 30 °C, Table 3, shows that the degree of oxygen loss is very similar in both cases, despite the removal of more charge (lithium), the additional

Table 3
Charge capacities associated with 4.5 V plateau for Li doped materials

Li doping level/y	Observed charge capacities associated with plateaux in Fig. 2 (mA h g^{-1})	Theoretical charge capacities based on amount of Li removed (chemical analysis) (mA h g^{-1})	Mn oxidation states from XPS	Compositions at end of plateau on charge
0.1	75	67	4	$Li_{0.23}H_{0.1}Mn_{0.88}O_{1.92}$
0.2	134	143	4	$Li_{0.24}H_{0.08}Mn_{0.82}O_{1.80}$

Li loss is compensated by H exchange. These values are in good agreement with the capacities associated with the two regions identified in Fig. 4.

In order to investigate structural changes during charge, powder neutron diffraction data were obtained for samples of $Li_xMn_{0.8}Li_{0.2}O_2$ charged to 4.5 and 4.8 V at 30 °C and 4.8 V at 55 °C. Rietveld refinement of the data from the sample charged to the start of the 4.5 V plateau gave an excellent fit to a single phase adopting the O3 structure (Fig. 5(a)) with lattice parameters $a = 2.850(1)$ Å, $c = 14.446(2)$ Å. This is consistent with the proposed conventional oxidation of Mn^{3+} to Mn^{4+}. Attempts to fit the data obtained from either sample charged to 4.8 V to a single phase model gave unsatisfactory results. For the sample charged at 30 °C an excellent fit was obtained using a model involving two O3 phases (Fig. 4(b)) having lattice parameters corresponding to: (1) the same as that obtained at 4.5 V and (2) a phase with similar a parameter (2.852(2) Å) and longer c parameter (14.646(6) Å). The observed similarity in a parameters is to be expected since this has a strong correlation with Mn oxidation state (4+ in both cases). From our previous diffraction studies of a wide range of doped and undoped layered lithium manganese oxides, both as-prepared and after electrochemical cycling, the elongated c parameter in phase B points to a material of the form $Li_xMn_yO_2$, where $y \sim 1$ [19–22]. Such a material is exactly what would be expected to result from loss of Li_2O.

The data obtained from the sample charged to 4.8 V at 55 °C again cannot be fitted to a single phase. A model involving two O_3 phases gives a much better fit to the data. However comparing the two data sets (30 and 55 °C) it is clear that for

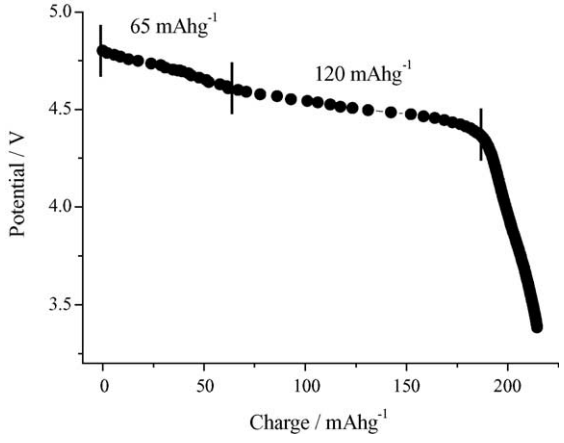

Fig. 4. Variation of potential (vs. Li^+[1 M]/Li) with state of charge for $Li_x[Mn_{1-y}Li_y]O_2$, $y = 0.2$, on the first charge at 25 mA g^{-1} (C/8) and 55 °C.

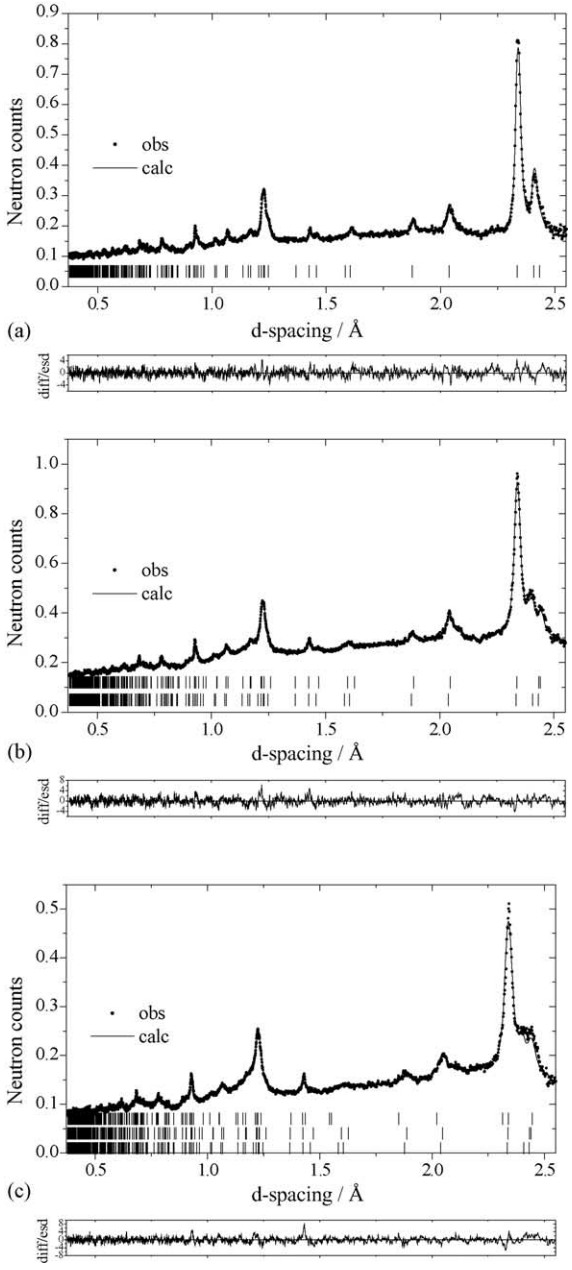

Fig. 5. Profile fits for Rietveld refinement of $Li_xMn_{0.8}Li_{0.2}O_2$. (a) charged to 4.5 V at 30 °C (single O3 phase model), (b) charged to 4.8 V at 30 °C, model incorporating two O3 phases, (c) charged to 4.8 V at 55 °C, model incorporating two O3 phases and one P3 phase. Dots indicate observed data, solid line calculated profile. The lower box shows difference/E.S.D.

the latter there is greater intensity at a d-spacing of around 2.45 Å. This corresponds well to the most intense 1 0 1 reflection of a phase with the P3 structure (AABBCC stacking, CrOOH structure type). A three phase model involving two O3 phases and a single P3 phase was tested and found to give an excellent fit (significantly better than that obtained for two O_3 phases) (Fig. 5c), in keeping with the proposed proton exchange mechanism favored at high temperatures.

The processes involved in charging $Li_xMn_{1-y}Li_yO_2$ may now be summarised. Initially Li is extracted accompanied by Mn oxidation until all Mn is in the 4+ oxidation state. Thereafter further Li is removed at 4.5 V which lies within the oxygen valence band and will result in oxidation of O^{2-}. This is unstable in the lattice leading to oxygen evolution (overall Li_2O removal). In addition, especially at higher states of charge, oxidation of the alkyl carbonates in the electrolyte yields H^+, as shown previously for other Li–Mn-oxides [8,9,23,24]. The H^+ will then exchange for Li^+.

Considering all our results on these three systems, there is clear evidence that in many cases both H^+ exchange and oxygen loss occur concurrently and the relative contributions of these processes to the extra "overcapacity" on charge can vary depending on conditions. Higher temperatures and higher states of charge both tend to favor proton exchange over oxygen (Li_2O) loss. Under ambient conditions it is the latter process that is the dominant source for the observed "overcapacity". It is known that H^+ is more prevalent in these electrolytes at 55 °C consistent with the greater role of exchange at this temperature. There is no net removal of charge from the electrode as it undergoes $Li^+ \leftrightarrow H^+$ exchange. The net effect of electrolyte oxidation generating H+ and e− then ion exchange is to reduce the Li content of the electrode. Considering the differences between the materials with and without Ni it is clear the Ni favours O loss. This is not surprising since O^{2-} in a Mn/Ni compound will be surrounded by both cations and both will be in the 4+ oxidation state. NiO_2 is a relatively unstable compound, readily evolving oxygen, hence we may conclude that O loss, when surrounded in part by Ni^{4+} instead of Mn^{4+}, is likely to be more facile as observed.

4. Conclusions

Higher temperatures (55 °C) promote more H^+ exchange for Li^+ than is the case at 30 °C for all three systems studied. For Li_2MnO_3 at 55 °C all the Li extracted (1.4 Li) is compensated for by H^+ exchange due to electrolyte oxidation. At 30 °C a mixture of O loss and H^+ exchange compensate for the Li extracted. For $Li_xMn_{1-y}Li_yO_2$ again both O loss and H^+ exchange occur alothough the former dominates. For $Li[Ni_xLi_{1/3-2x/3}Mn_{2/3-x/3}]O_2$ O loss is by far the dominant mechanism although there is some H^+ exchange especially at 55 °C. The dominance of O loss in the Ni containing compound can be understood in the light of the relative ease with which NiO_2 will lose oxygen. Where O loss dominates this is explained not by the diffusion of O in the lattice but by the loss of O at the surface and diffusion of the cations into the centre of the particle occupying sites once occupied by Li.

Acknowledgements

PGB is indebted to the Royal Society, the EU and the EPSRC for financial support.

References

[1] B. Ammundsen, J. Paulsen, Adv. Mat. 13 (2001) 943.
[2] M. Tabuchi, H. Shigemura, K. Ado, H. Kobayashi, H. Sakaebe, H. Kageyama, R. Kanno, J. Power Sources 97–98 (2001) 415.
[3] P. Kalyani, S. Chitra, T. Mohan, S. Gopukumar, J. Power Sources 80 (1999) 103.
[4] M.N. Richard, E.W. Fuller, J.R. Dahn, Solid State Ionics 73 (1994) 81.
[5] Z. Lu, J.R. Dahn, J. Electrochem. Soc. 149 (2002) 815.
[6] Z. Lu, D.D. MacNeil, J.R. Dahn, Electrochem. Solid State Lett. 4 (2001) 191.
[7] Z. Lu, L.Y. Beaulieu, R.A. Donaberger, C.L. Thomas, J.R. Dahn, J. Electrochem. Soc. 149 (2002) A778.
[8] A.D. Robertson, P.G. Bruce, J. Chem. Soc. Chem. Comm. (2002) 2790.
[9] A.D. Robertson, P.G. Bruce, Chem. Mater. 15 (2003) 1984.
[10] A.R. Armstrong, P.G. Bruce, Electrochem. Solid State Lett. 7 (2004) 1.
[11] A.D. Robertson, P.G. Bruce, Electrochem. Solid State Lett. 7 (2004) A294.
[12] J.C. Matthewman, P. Thompson, P.J. Brown, J. Appl. Crystallogr. 15 (1982) 167.
[13] P.J. Brown, J.C. Matthewman, Rutherford Appleton Laboratory Report, RAL-87-010, 1987.
[14] V.F. Sears, Neutr. News 3 (1992) 26.
[15] K. Kanamura, S. Toriyama, S. Shiraishi, Z. Takehara, J. Electrochem. Soc. 143 (1996) 2548.
[16] Y. Paik, C.P. Grey, C.S. Johnson, J.S. Kim, M.M. Thackeray, Chem. Mater. 14 (2002) 5109.
[17] J.S. Kim, C.S. Johnson, J.T. Vaughey, M.M. Thackeray, S.A. Hackney, W. Yoon, C.P. Grey, Chem. Mater. 16 (2004) 1996.
[18] W.-S. Yoon, Y. Paik, X.-Q. Yang, M. Balasubramanian, J. McBreen, C.P. Grey, Electrochem. Solid State Lett. 5 (2002) 263.
[19] A.D. Robertson, A.R. Armstrong, P.G. Bruce, J. Chem. Soc., Chem. Comm. (2000) 1997.
[20] A.D. Robertson, A.R. Armstrong, A.J. Fowkes, P.G. Bruce, J. Mater. Chem. 11 (2001) 113.
[21] A.R. Armstrong, A.J. Paterson, A.D. Robertson, P.G. Bruce, Chem. Mater. 14 (2002) 710.
[22] A.R. Armstrong, N. Dupre, A.J. Paterson, C.P. Grey, P.G. Bruce, Chem. Mater. 16 (2004) 3106.
[23] A. Du Pasquier, A. Blyr, P. Courjal, D. Larcher, G. Amatucci, B. Gérand, J.-M. Tarascon, J. Electrochem. Soc. 146 (1999) 428.
[24] M. Moshkovich, M. Cojocaru, H.E. Gottlieb, D. Aurbach, J. Electroanal. Chem. 497 (2001) 84.